Vision Research 49 (2009) 2902–2910

Contents lists available at ScienceDirect

Vision Research

journal homepage: www.elsevier.com/locate/visres

Illusory position shift induced by plaid motion

Rumi Hisakata *, Ikuya Murakami

Department of Life Sciences, University of Tokyo, Tokyo, Japan

ARTICLE INFO

Article history:
Received 11 May 2009
Received in revised form 3 September 2009

Keywords:
Illusory position shift
Motion integration
Plaid motion

ABSTRACT

In the motion-induced position shift (MIPS), the position of a moving pattern tapered by a stationary envelope is perceived to shift in the direction of the motion. It was found that plaid motion also elicited a MIPS in the direction of global motion and this global MIPS could not be predicted by the average of the local MIPSs due to component motions. We also used a pseudo plaid pattern and again observed a global MIPS that could not be predicted by the local MIPSs due to the components of the pseudo plaid pattern. We suggest the possibility that the receptive-field positions of global motion detectors shift in the direction opposite to global motion, resulting in a positional displacement in activation via population coding.

1. Introduction

The localization of object position represents one of the most important human visual processing abilities. We can correctly identify the position of a stationary target in reference to stable landmarks and detect the misalignment between two targets with very high precision (e.g. Braddick, 1984; Carney & Klein, 1999; Morgan, Ward, & Hole, 1990; Patel, Bedell, & Ukwade, 1999; Westheimer, 1975). However, the position of a moving object is often perceptually mislocated in various ways (for a review see Whitney, 2002). For example, in the flash-lag effect, a flashed stimulus is perceived as lagging behind a moving stimulus (Nijhawan, 1994, 1997). In addition, if a flashed stimulus is accompanied by a large moving context in its vicinity, the flash appears to be displaced in the direction of the neighboring motion. Although these phenomena indicate that significant interactions must occur between position coding and motion processing, the mechanisms underlying the position coding of moving and stationary objects remain unclear.

Motion-induced position shift (MIPS) is a phenomenon in which a stationary contour defining a coherently moving texture appears to shift in the direction of motion (De Valois & De Valois, 1991; Ramachandran & Anstis, 1990). De Valois and De Valois (1991) showed that a moving Gabor patch comprised of a drifting sinusoidal carrier and a stationary Gaussian envelope was perceptually displaced in the direction of motion. The extent of mislocalization depended on both the spatial and temporal frequencies of the Gabor patch. Following these results, the MIPS has been investigated in many experimental paradigms, as summarized below.

This illusion has several characteristics. First, the MIPS does not occur if the stationary contour of a moving stimulus has a sharp edge. It is necessary to use blurry or ambiguous contours (Arnold, Thompson, & Johnston, 2007; Whitney et al., 2003). Second, the extent of MIPS depends on speed and duration (Chung, Patel, Bedell, & Yilmaz, 2007; McGraw, Whitaker, Skillen, & Chung, 2002; Tsui, Khuu, & Hayes, 2007a, 2007b). Third, the MIPS occurs for many kinds of motion, including first-order motion (De Valois & De Valois, 1991), second-order motion (Bressler & Whitney, 2006), random-dot kinematograms (Ramachandran & Anstis, 1990), motion-defined motion (Durant & Zanker, 2009), three-dimensional motion (Edwards & Badcock, 2003; Tsui et al., 2007a), global motion (Mussap & Prins, 2002; Rider & Johnston, 2009), and the motion defined by binocular correlations (Murakami & Kashiwabara, 2009). The MIPS also occurs in a stationary stimulus after adaptation to motion, in the direction opposite to that of the adapting stimulus (McGraw et al., 2002; Nishida & Johnston, 1999; Snowden, 1998). Fourth, the MIPS occurs after motion adaptation even when the crowding effect prevents the observer from recognizing the direction of the adapting stimulus, suggesting the involvement of a preattentive process (Harp, Bressler, & Whitney, 2007; Whitney, 2005). These previous studies clarify that MIPS is elicited in the presence of various motion stimuli and percepts.

Possible underlying mechanisms of the MIPS have been proposed. The first possibility involves feedback connections from a higher processing stage (e.g., area MT) specialized for motion to a lower stage (area V1 or V2) responsible for precise position coding (Arnold et al., 2007; Durant & Johnston, 2004; Nishida & Johnston, 1999). For example, Nishida and Johnston (1999) showed that after adaptation to rotation, a stationary windmill pattern appeared to incline in the direction of motion aftereffect. Because rotation is

* Corresponding author. Address: c/o Murakami Lab, Department of Life Sciences, University of Tokyo, 3-8-1 Komaba, Meguro-ku, Tokyo 153-8902, Japan. Fax: +81 3 5454 6979.
E-mail address: hisakata@fechner.c.u-tokyo.ac.jp (R. Hisakata).

0042-6989/$ - see front matter © 2009 Elsevier Ltd. All rights reserved.
doi:10.1016/j.visres.2009.09.009

thought to be processed in a higher stage, the authors suggested that interactions between lower and higher areas through abundant recurrent inputs from area MT to V1 and V2 (Bullier, 2001; Shipp & Zeki, 1989a, 1989b) are involved in the MIPS. The second possibility is that the position coding related to the MIPS independently exists at several hierarchical processing stages. Bressler and Whitney (2006) and Pavan and Mather (2008) found that second-order motion induces MIPS and suggested that, because first- and second-order motions are presumably processed by different mechanisms (e.g. Derrington, Badcock, & Henning, 1993; Nishida & Sato, 1995), each type of motion might induce an independent MIPS. The third possibility involves an attentionally accessible spatial map located at a higher-order stage (Shim & Cavanagh, 2004; Watanabe, Nijhawan & Shimojo, 2002).

Considering the functional stages, it is still an open question as to where the underlying mechanism of the MIPS is located in visual processing. It is widely known that the cortical processing of color and motion involves a hierarchy, or multiple stages (e.g. Bradley & Goyal, 2008; Gegenfurtner, 2003; Solomon & Lennie, 2007), and a few psychophysical attempts have been made to identify the responsible mechanism in this hierarchy. Hayes (2000) showed that contour detection perception was influenced by the perceived position due to MIPS, not by the retinal positions of the contour elements, suggesting that the mechanisms underlying the MIPS is located at some early processing stage. Also, Murakami and Kashiwabara (2009) reported a MIPS induced by the motion defined by binocular correlation, suggesting that the underlying mechanism of the MIPS is located at a binocular stage.

To examine whether the MIPS occurs in the presence of a particular kind of motion is a promising approach for identifying the cortical locus of the MIPS in relation to the hierarchical cortical processing of visual motion. In this respect, plaid is a useful stimulus for investigating the relationship between a particular visual phenomenon and the process by which visual motion is integrated. The plaid stimulus is the linear sum of two sinusoidal gratings with different orientations in the same position of the visual field (Adelson & Movshon, 1982). When the superimposed pair of moving sinusoidal gratings has the same luminance contrast, spatial frequency, and temporal frequency, one usually perceives coherent global motion rather than transparent motion by two component gratings. The perceived global motion is consistent with either the vector sum of the directions of the component motions or the intersection of the two constraint lines about possible directions of global motion (Adelson & Movshon, 1982; Bowns, 1996; Burke, Alais, & Wenderoth, 1994; Kim & Wilson, 1993; Welch, 1989). At least two sequential stages should be involved in the visual processing of plaid motion, namely detecting component motions and integrating them (Welch, 1989). By using the plaid motion as a stimulus for psychophysical experiments on MIPS, we can examine the relationship between the mechanisms underlying the MIPS and the hierarchy of motion information processing, and we can discuss the process of position coding for moving objects.

The superimposition of two gratings with different orientations looks like a crosshatched texture containing many intersections between two stripes. Because the luminances of the two components are additive, these intersections have the maximal luminance contrast. Therefore, simple rectification could transform luminance to the second-order (contrast) energy that is consistent with the direction of the global motion (Burke et al., 1994; Derrington et al., 1993; Kim & Wilson, 1993). In addition, a feature-tracking mechanism could monitor the movements of these contrast maxima in the direction of global motion (Bowns, 1996). To rule out any contribution of these second- and third-order motion systems, researchers frequently use a pseudo plaid pattern (Amano, Edwards, Badcock, & Nishida, 2009; Nishida, Amano, Edwards, & Badcock, 2006; Takeuchi, 1998). This stimulus consists of multiple Gabor patches with different orientations, all of which are drifting at a speed that is consistent with a single global motion (see Section 3.1).

If plaid motion induces a MIPS in the direction of the global motion, this would constitute straightforward evidence for motion-mediated position coding after motion integration. We investigated whether MIPS was induced by a plaid comprised of the superposition of two sinusoids with different orientations (Experiment 1). When moved within a stationary contrast envelope, the plaid appeared to shift in the global motion direction, rather than in the oblique directions in which the two component gratings of the plaid were drifted. The magnitude of MIPS could not be predicted by a combination of the MIPSs due to the component gratings of the plaid. However, as mentioned above, this plaid contained the second-order and feature-tracking motions in the same direction as the global motion. To reject the involvement of these motions, we also used a pseudo plaid pattern, which consisted of multiple small Gabor patches of random orientations, without spatial overlap between patches (Experiment 2). It was found that the pseudo plaid pattern also induced global MIPS, rather than a mixture of locally jittering MIPSs due to local Gabor patches, and that the magnitude of the lobal MIPS could not be predicted by the MIPSs that might be induced by the local Gabor patches.

2. Experiment 1

2.1. Methods

2.1.1. Observers

One of the authors (RH) and four observers with normal or corrected-to-normal vision participated (aged 19–24 years). Except RH, they were naive to the objective of this experiment. Observers viewed the stimuli binocularly from a distance of 85.9 cm.

2.1.2. Apparatus

Stimuli were generated by a computer (Apple PowerMac G4) and were displayed on a CRT monitor (iiyama NM204D, 1600 × 1200 pixels, 1 min/pix, refresh rate 75 Hz), which was gamma-corrected with a 10-bit-depth color look-up table on a videocard.

2.1.3. Stimuli

Two identical stimuli appeared above and below a fixation point and moved in opposite directions (Fig. 1a). We presented four types of stimuli (Fig. 1b):

- (VG) a vertical grating blurred by a Gaussian contrast envelope with a s.d. of 24 min, carrier spatial frequency of 5 cpd, and speed of 0.8 deg/s;
- (Plaid) the linear sum of two superimposed component gratings of identical envelope size, luminance contrast, and carrier spatial frequency as VG, but having different orientations as designated below;
- (CG1) only one component grating of the Plaid presented separately;
- (CG2) only the other component of grating of the Plaid presented separately.

The Michelson contrast was 99% for all stimuli, and the background was maintained at the mean luminance (49.5 cd/m^2). The carrier of each stimulus was drifted within the stationary Gaussian envelope. The VG moved to the left or right at 0.8 deg/s. There were three conditions for the Plaid. The component gratings of the Plaid were moved in the directions of ±22.5°, ±45°, or ±67.5° (hereafter referred to as the plaid-angles), with 0° indicating the horizontal

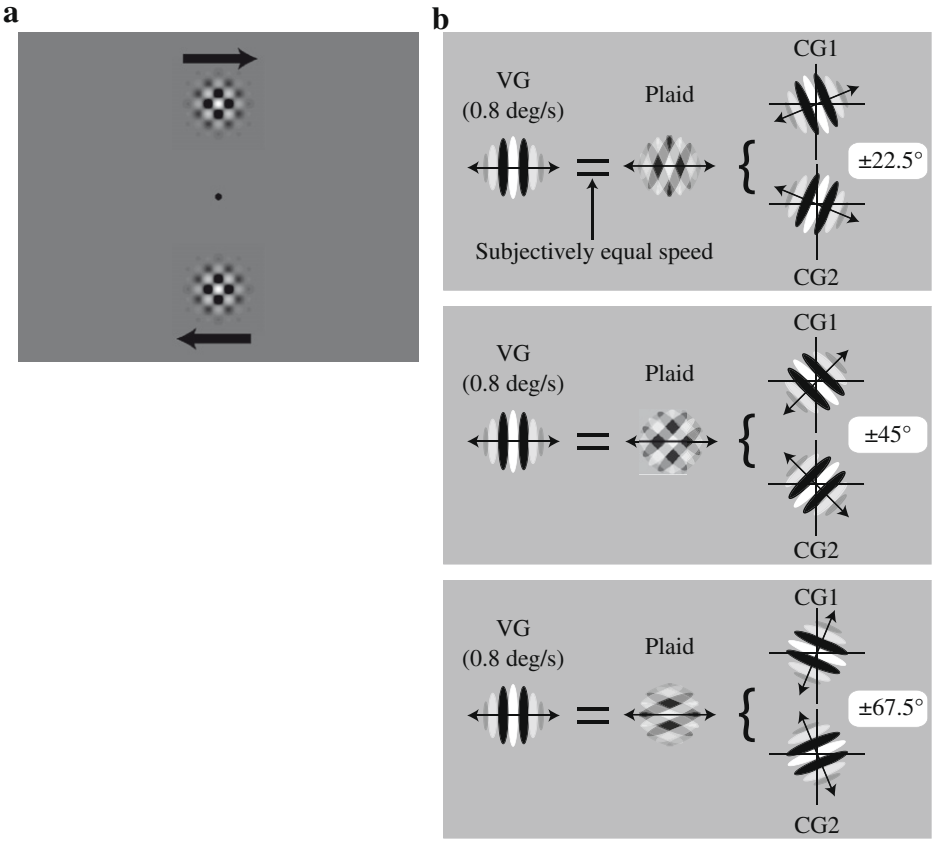

Fig. 1. The stimulus configuration in Experiment 1. a: A snapshot of typical stimuli. The filled circle in the middle is the fixation point. The black arrows schematically indicate the perceived directions of motions of the upper and lower patterns. b: The four types of stimuli and the three plaid-angle conditions. Each panel indicates each plaid angle condition.

direction. All of these conditions yielded perception of global motion in a horizontal direction under the experimental conditions. The center-to-center distance between the fixation point and each stimulus was 4 deg.

Because the MIPS is known to be induced by perceived motion (e.g. McGraw et al., 2002), we considered it necessary to equate the perceived speed of stimuli before comparing illusion strength across different motion conditions. In a preparatory experiment, we determined the speed of each Plaid that was subjectively equal to the VG moving at 0.8 deg/s. Each session of this preparatory experiment was continued until 10 reversals of staircase occurred in the standard procedure of the staircase method, and the average of the last four reversal points was determined as the point of subjective equality. The average of the subjectively equal speeds for four such sessions was used in the main experiment. Under all conditions of plaid-angles, the speed of the Plaid was subjectively equated to that of the VG at 0.8 deg/s for each observer. Therefore, whereas the speed of the VG was set at 0.8 deg/s, the speeds of the other stimuli were variable across observers (on average, the physical speeds of the Plaids at the point of subjective equality were 0.88, 0.94, and 1.08 deg/s under the ±22.5°, ±45° and ±67.5° plaid-angle conditions respectively). Whereas the Plaid appeared to move as fast as the VG, the CG1 and CG2 appeared generally slower than the VG because they were the single presentations of the two components of the Plaid.

2.1.4. Procedure

One second after the fixation point appeared at the center of the monitor, two stimuli of an identical type were presented simultaneously in the upper and lower portions of the visual field for 1 s (Fig. 1a). The upper and lower stimuli moved in directions opposite from each other. The observer's task was to judge whether the upper stimulus was displaced to the left or to the right of the lower stimulus. The four types of stimuli (VG, Plaid, CG1, and CG2) were presented in random order within each session, and the three plaid-angle conditions (22.5°, 45°, and 67.5°) were randomized across sessions. The MIPS was quantified by the point of subjective alignment between the two stimuli using the method of constant stimuli with 30 repeated trials per point. Each psychometric curve was fitted with the cumulative Gaussian function. Because no systematic difference in the size of MIPS emerged whether the upper stimulus moved right and the lower stimulus moved left or vice versa, we averaged the data for these two mirror-symmetrical conditions.

2.2. Results and discussion

The MIPSs under all conditions were plotted in Fig. 2 for each observer separately. For the vertical grating (VG), we obtained reliable MIPS, consistent with the original study by De Valois and De Valois (1991). While the magnitude measurements of MIPS for VG were statistically highly significant (as indicated by small error bars) across conditions, the absolute value of illusory displacement showed considerable across-observer variability.

The Plaid, or the linear sum of two component gratings having the orientations of ±22.5°, ±45°, or ±67.5°, always appeared to move coherently to the left or right. As in the case of the VG, the Plaid also yielded a statistically significant MIPS (the bootstrap

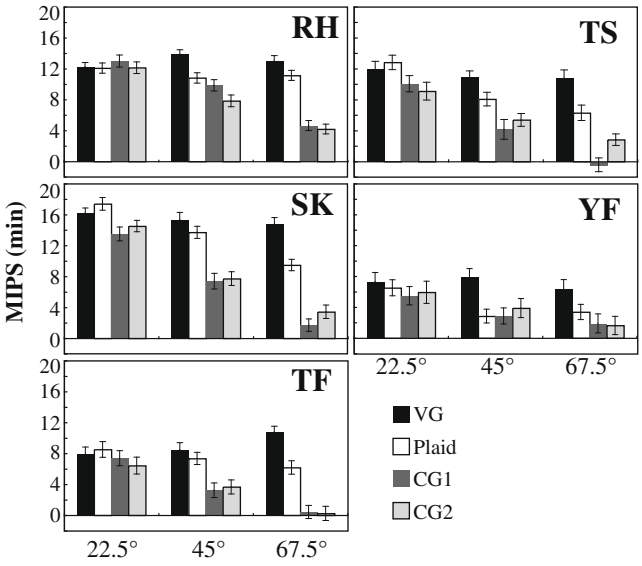

Fig. 2. The results of Experiment 1. The extent of MIPS, i.e., the point of subjective alignment, is plotted for the five observers in separate panels. The error bars indicate the standard errors estimated by the bootstrap method (with 10^4 iterations).

method, $p < .01$) in the direction of global motion under all plaid-angle conditions. The extent of MIPS in the Plaid was either comparable to or weaker than the MIPS observed in the VG.

When we separately presented only one of the two component gratings (CG1 and CG2) of the Plaid, the magnitude became significantly smaller as plaid-angle increased (ANOVA, $F(2, 8) = 24.66$, $p < .001$). For the 22.5° plaid angle, there was only a small difference in the magnitude of MIPS between the Plaid and the component gratings (CG1 and CG2). For the 45° plaid angle, the difference became more obvious for some observers (SK and TF) but not for others. However, the 67.5° plaid angle clearly showed an interesting pattern: the MIPS for the Plaid was much greater than those for CG1 and CG2 (Ryan's multiple comparison test, $t(36) = 6.69$, $p < .05$ for CG1 and $t(36) = 5.73$, $p < .05$ for CG2).

When the CG1 or CG2 was presented separately, what each observer actually saw was a single obliquely oriented grating moving orthogonally. Thus, just as the VG led to a MIPS along the horizontal axis, the MIPS for the CG1 and CG2 should occur in the oblique direction in which they appeared to move. Nonetheless, we forced each observer to judge the horizontal displacement between the upper and lower stimuli, so we were actually measuring the horizontal component of the MIPS in the oblique direction. Therefore, the magnitude of "MIPS" in Fig. 2 should be the orthogonal projection of the true MIPS in the oblique direction onto the horizontal axis of space. Also, to obtain the same global speed, the physical speed of each component grating should be decreased as the plaid-angle increased (Adelson & Movshon, 1982) and actually the speeds of the component gratings of the Plaid that was speed-matched to the VG decreased with increasing plaid-angle. Hence the resulting "MIPS" in Fig. 2 should also decrease, assuming the dependence of MIPS on stimulus speed (Chung et al., 2007; McGraw et al., 2002; Tsui et al., 2007a). Therefore, the decrease in the "MIPS" for the CG1 and CG2 as a function of plaid angle was predicted (see Appendix A).

The real question here was whether the MIPS profile obtained for the Plaid could be explained by a combination of the MIPSs for the CG1 and CG2 or by the global motion perceived in the same speed irrespective of plaid-angles. If MIPS is induced by global motion, not by component gratings, the magnitude of MIPS will stay constant regardless of plaid angles. On the other hand, if MIPS is induced only by component gratings, the magnitude of MIPS will decrease as the plaid-angle decreases. The mean of the MIPSs for the CG1 and CG2 was plotted together with the MIPS for the Plaid (Fig. 3). Except for observer YF's data, it was evident that the mean MIPS could not explain the MIPS for the Plaid in most cases, especially for 67.5° plaid angle. Neither could the sum of the MIPSs for the CG1 and CG2 (i.e., twice the mean MIPS), because it was greater than the MIPS for the Plaid in 22.5° plaid angle and smaller in 67.5° plaid angle. On the other hand, the MIPS obtained for the Plaid appeared to be constant across different plaid-angles. Based on this pattern of results, we concluded that the MIPS seen in the Plaid did not simply reflect the MIPSs elicited by its component gratings.

The implication of the present results is that the mechanism underlying the MIPS exists in some higher stage of visual motion processing hierarchy where the representation of global motion of the plaid is made explicit. However, the plaid used in the present experiment contains several different cues to global motion. The first cue is luminance-based first-order motion information from which the true motion can be estimated by using the intersection-of-constraints rule or vector-summation rule. The second cue is the profile of luminance contrast that moves in the same direction as above and that is visible by second-order motion processing (Derrington et al., 1993; Kim & Wilson, 1993). The third cue resides in highly salient luminance peaks at intersections that might be used by a feature-tracking mechanism as third-order motion information (Lu & Sperling, 1995; Sperling, 1998). Indeed, Bressler and Whitney (2006) showed that second-order motion defined by contrast modulation induced MIPS. On the basis of these studies, the possibility remains that these second and third cues to motion, rather than global motion computed from two independent first-order motion components, contributed to the MIPS observed in Experiment 1.

Previous psychophysical studies on global motion computation have made use of several types of pseudo plaid patterns having no spatial overlap of local motion components. Human observers clearly perceive coherent motion in these patterns (Amano et al., 2009; Nishida et al., 2006; Takeuchi, 1998). In Experiment 2, we examined whether MIPS could be induced by a pseudo plaid pattern without second-order contrast-defined motion or moving trackable features.

3. Experiment 2

3.1. Methods

3.1.1. Observers

One of the authors (RH) and three naive observers who had already experienced Experiment 1 participated.

3.1.2. Apparatus

Stimuli were generated by a computer (Apple MacPro) and were displayed on a CRT monitor (Mitsubishi Electric RDF223H, 1600 × 1200 pixels, 1 min/pix, refresh rate 75 Hz, mean luminance 48 cd/m^2).

3.1.3. Stimuli

We used a pseudo plaid pattern (PPP) (Amano et al., 2009): 21 local Gabor patches were arranged in a regular 0.8 deg × 0.8 deg grid (Fig. 4) and their carrier gratings had random orientations. The envelope s.d. of each local patch was 9 min, the carrier's spatial frequency was 2 cpd, and the Michelson contrast was 80%. The orientation and spatial phase of each local patch was randomized, and the drift speed was consistent with a common global motion, such that the speed was varied according to the sine function of the angle between the orientation of each patch and the direction of the

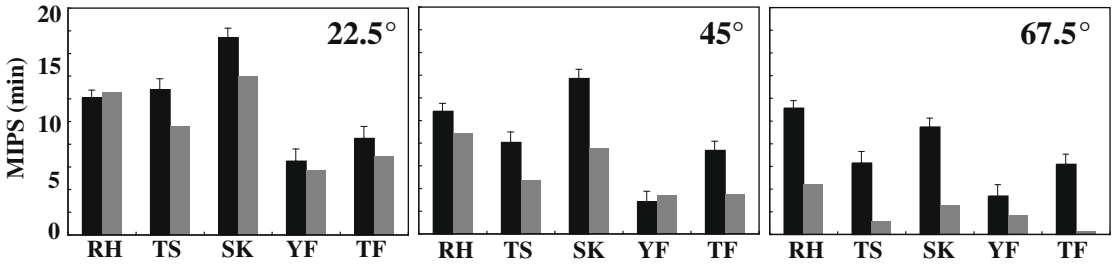

Fig. 3. Comparison between the measured MIPS for the Plaid (black bars) and the average of the predicted MIPSs (gray bars) that would be induced by the two component gratings (CG1 and CG2) of the Plaid.

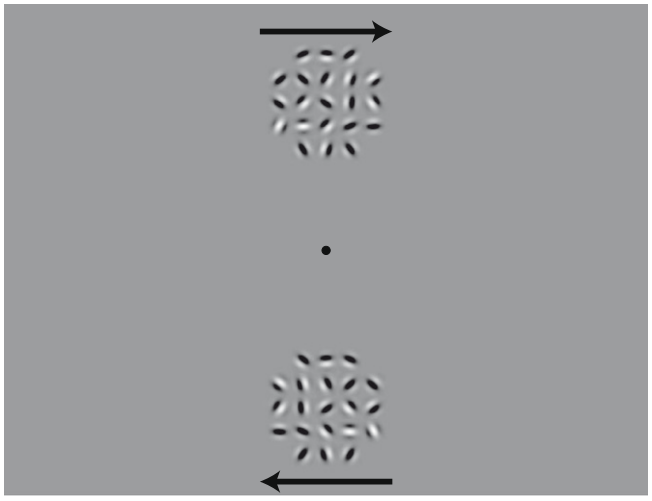

Fig. 4. The stimulus configuration in Experiment 2. The filled circle in the middle is the fixation point. The black arrows schematically indicate the perceived directions of motions of the upper and lower patterns.

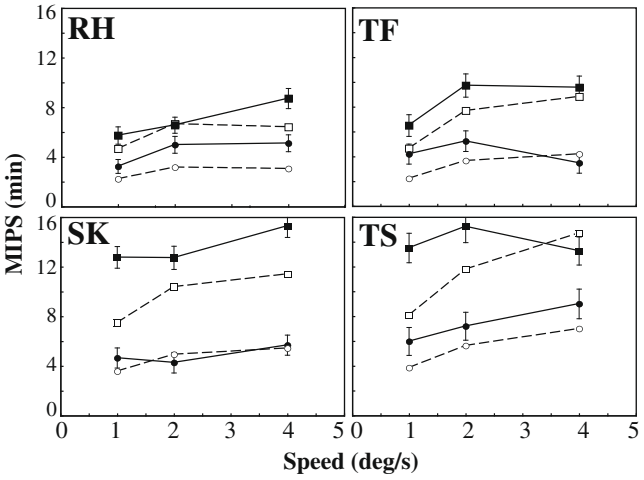

Fig. 5. The results of Experiment 2. The extent of MIPS is plotted for the four observers in separate panels. In each panel, the MIPS is plotted against the speed of global motion. The error bars indicate the standard errors estimated by the bootstrap method (with 10^4 iterations). The filled squares and circles indicate the MIPSs for full and half signal conditions respectively. The open symbols and dashed lines indicate the predicted MIPS; the square and circle symbols indicate the full and half signal condition.

global motion. The global motion was either leftward or rightward. Two such PPPs were presented simultaneously in the upper and lower portions of the visual field and were moved in opposite directions from each other. The distance between the fixation point and the center of each PPP was 6 deg.

To change the perceived speed of PPP, we manipulated the global-motion speed and the signal-to-noise ratio. We used three global-motion speeds: 1, 2, and 4 deg/s. Since Amano et al. (2009) showed that the perceived speed of the PPP decreased with decreasing signal-to-noise ratio, we attempted to manipulate perceived speed by varying the signal-to-noise ratio independently of the physical global-motion speed. We tested two levels of signal-to-noise ratio, full and half. Under the full signal condition, all 21 local patches moved according to the sine law as described above, whereas under the half signal condition, only 10 local patches obeyed the sine law and the other 11 local patches moved at random speeds within the range of ±1, ±2, or ±4 deg/s at each global-motion speed.

3.1.4. Procedure

A fixation point appeared at the center of the monitor for 1 s, followed by a 500-ms presentation of two PPPs. Each observer judged whether the position of the entire upper PPP was to the left or to the right of the entire lower PPP. In all other respects, the procedure and analysis were identical to those used in Experiment 1.

3.2. Results and discussion

Fig. 5 shows the extent of MIPS for the PPP (filled symbols with solid lines). Roughly constant values of standard errors indicate that the same positional discriminability was maintained across speed conditions. Again, it was confirmed by each observer's introspection that each pattern appeared to move coherently in the same direction rather than to move chaotically in random directions.

Under all conditions, significant MIPSs were obtained for all observers (the bootstrap method, $p < .01$). This result is consistent with the studies that examined the MIPS induced by random dots (Mussap & Prins, 2002) and by an array of local motions (Rider & Johnston, 2009). The magnitude of MIPS increased with increasing physical global-motion speed (ANOVA, $F(2, 6) = 6.04$, $p < .05$), however individual differences also seemed to emerge. For all observers, the MIPS under the full signal condition was greater than that under the half signal condition (ANOVA, $F(1, 3) = 17.00$, $p < .05$). A positive correlation between perceived speed and MIPS was seen as we manipulated each of the two dimensions, namely physical global-motion speed and signal-to-noise ratio, though a more objective confirmation is needed to draw a firm conclusion.

As in Experiment 1, we examined whether the MIPS for the PPP could be predicted by the average of MIPSs for local Gabor patches. For this purpose, the MIPS for a single local Gabor patch was measured at three motion speeds (1, 2, and 4 deg/s) in a subsidiary experiment. A single Gabor patch, whose size and spatial frequency were the same as those of each local patch of the PPP, was presented at 6 deg eccentricity from the fixation point. As in the main experiment, two such Gabor patches were displayed in the upper and lower portions of the visual field for

500 ms, and the point of subjective alignment was determined. The MIPS for the local Gabor patch determined for observers RH, SK, TF, and TS was 9.32, 14.98, 9.31, and 16.16 min, respectively, at 1 deg/s; at 2 deg/s, 11.85, 18.20, 14.50, and 21.12 min; at 4 deg/s, 9.44, 18.43, 14.24, and 25.21 min. On the basis of these values, we predicted how much MIPS along the horizontal axis should occur if any one of the local patches of the PPP were presented alone (see Appendix B). The average of the predicted "local MIPSs" for all the 21 local patches was used as the prediction. Because the orientations of the local patches were chosen randomly in the experiment, the predicted MIPS was calculated using a stochastic simulation with 10^5 repeats. Fig. 5 compares the predicted MIPS (open symbols with dashed lines) with the measured MIPS. Under the full signal condition, the measured MIPS was greater than the predicted MIPS, except for observer RH at 2 deg/s and observer TS at 4 deg/s. Under the half signal condition, the measured MIPS also exceeded the prediction, except for observer SK at 2 deg/s and observer TF at 4 deg/s. The actual MIPS was significantly greater than the local prediction ($t(23) = 4.96$, $p < .05$). Therefore, the average of local MIPSs could not explain the measured global MIPS.

We also examined whether the maximum of the local MIPSs could predict the global MIPS. As a result of a stochastic simulation, the maximum local MIPS averaged across speed conditions was 10.14, 17.09, 12.59, and 20.67 min for observers RH, SK, TF, and TS, respectively, under the full signal condition, and was 10.27, 16.83, 12.40 and 20.31 min for the above four observers under the half signal condition. These predictions contradicted the actual data and the difference was significant ($t(23) = 8.20$, $p < 0.01$). Additionally, we examined whether the global MIPS was equal to the median of the local MIPSs. To avoid the statistical risk that the average and the maximum are susceptible to an outlier, the visual system might take the median as a more conservative solution. However, it could not predict the global MIPS ($t(23) = 2.80$, $p < .05$).

A local motion signal that somehow captured one's attention might determine the global MIPS. However, the most likely candidate for the moving patch capturing one's attention would be the fastest motion of all patches, i.e., the maximum hypothesis proposed in the previous paragraph, which was shown to be wrong. In addition, we did not see the fastest patch pop out in the PPP, and also we could individuate neither the fastest local patch, nor any local patch, at 6 deg eccentricity, but simply saw the pattern move as a whole. According to these observations, it is unlikely that attention could identify any conspicuous local patch from a crowd of patches.

4. General discussion

4.1. Summary of the experiments

In Experiment 1, we found that plaid motion also induces a motion-induced position shift (MIPS). The MIPS in response to the plaid could not be predicted from the average of the local MIPSs and the magnitude of MIPS appeared to be constant regardless of plaid-angles. To exclude the possibility that the second-order motion or feature-based motion induced a position shift, a pseudo plaid pattern (PPP) was used in Experiment 2 and again resulted in an illusory position shift. In this case also, the MIPS increased with the perceived speed of PPP and the extent of the global MIPS could not be predicted by the average of the MIPSs that would occur in local patches if each of them were presented alone. These results clearly indicate the existence of a mechanism that processes position and that is susceptible to motion representation at the stage of motion integration.

4.2. Relationship with previous studies

Mussap and Prins (2002) previously demonstrated that "global motion" could induce a MIPS. In their study, a stationary or dynamic random-dot pattern within a blurred contrast envelope appeared to shift in the direction of the coherent motion superimposed on the non-moving pattern. The coherently moving dots within and outside of the envelope could induce a positional shift in the central random-dot pattern, and a high-pass-filtered version of a stimulus also elicited the same illusion. Therefore, the researchers argued that a motion representation after the process of motion integration influences perceived position. Our study is largely consistent with their proposal in that position perception can be influenced by higher-order motion processing, presumably accomplished by neurons in area MT or MST (see below), but the critical difference is that we used a different kind of global motion from that used in the previous study. Mussap and Prins used coherently moving dots, each of which contained first-order motion energy (or second-order contrast-based energy in their high-pass version) in the direction of global motion: in other words, component signal motions and integrated motion moved in the same direction. In clear contrast, our stimulus contained two (in Experiment 1) or many (in Experiment 2) different component directions, from which one global velocity had to be integrated. Studies have shown that different perceptual properties emerge in response to different types of global motion stimuli (Scase, Braddick, & Raymond, 1996), and there is abundant evidence that MT neurons preferring coherent global motion do not necessarily exhibit global motion ("pattern-motion") selectivity in response to stimulation by plaids (Born & Bradley, 2005; Majaj, Carandini, & Movshon, 2007; Movshon & Newsome, 1996). Recently, single MT neurons have been shown to exhibit pattern-motion selectivity for the overlapping conventional plaid but not for the non-overlapping pseudo plaid pattern (Majaj et al., 2007). Thus, the MIPS observed in response to the PPP in the present study might require even higher-order computation for global motion involving population coding. In this respect, our finding sheds some light on possible processing links between motion and position.

A MIPS was also reported to occur in a local central region after motion adaptation in its surround (Whitney, 2005). The perceived position shift was in the direction opposite to the adapting motion. Whitney and Cavanagh (2000) showed that nearby motion also elicited an illusory position shift for a flashed stationary stimulus. These studies suggested that spatial pooling is involved in this illusion and that motion processing units with large receptive fields or long-range spatial propagations of motion signals along a retinotopic map are playing some critical role. Physiological evidence for the site of critical processing for the MIPS in humans has also been reported (McGraw, Walsh, & Barrett, 2004). A technique for transient cortical deactivation using transcranial magnetic stimulation demonstrated that the activities of MT, but not V1, were needed for the occurrence of the MIPS illusion. This finding is consistent with the suggestion of the aforementioned previous studies with regard to MIPS in response to large-scale motion stimulation. Evidence, including the results of the present study, supports the involvement of higher-order cortical motion processing in the MIPS illusion.

4.3. Why does the MIPS occur?

Do existing models for this illusion explain the global MIPS? Tsui et al. (2007b) and Chung et al. (2007) proposed a theory of biased centroid, in which the neural facilitation and attenuation in the direction of motion displace the centroid of the activation profile along the motion direction, and the perceived position of a moving stimulus is based on this shifted centroid. According to

this model, the apparent contrast (or neural activation level) of the leading portion of the moving Gabor patch is boosted while that of the trailing portion is attenuated. However, this model seems to be unable to explain our data in Experiment 2. We measured the extent of the MIPS for a single local Gabor patch at 6 deg eccentricity and found that the MIPS could be as large as 2 s.d. of the Gaussian window of the Gabor patch. To make this extent of displacement possible and for perceived contrast to remain the same, the physical contrast at 2 s.d. should be boosted by over 700%, which is biologically unlikely.

Fu, Shen, Gao, and Dan (2004) and Fu et al. (2002) found that the receptive fields of V1 neurons were shifted in the direction opposite to the motion direction. They argued that this receptive-field displacement was implemented as biased inputs from the presynaptic neurons. This direction-selective receptive-field shift should cause a perceptual shift of the stimulus position in the direction of motion, assuming a population-decoding scheme. A neuron whose receptive field is initially centered at a particular position of the visual field is assumed to convey visual information at this position. Now that this neuron has a shifted receptive field, it codes visual information from this shifted position as if coming from the original position. If all neurons exhibit the same amount of receptive-field shift, the resulting population coding of the outer visual event will shift the visual representation in the direction of motion. However, receptive-field shifts in V1 can explain only a local MIPS, i.e., small mislocalization of a small moving stimulus in the direction of local motion, but cannot explain the global MIPS.

What scheme might be postulated as an alternative? For a simple and easily implementable explanation, we propose that the receptive fields of a "global motion detector" are shifted in the direction opposite to global motion and induce a global MIPS. This motion detector should be in a higher stage of visual processing, for example area MT or MST, because spatially converging inputs are required; indeed, a subpopulation of neurons in these areas is selective for the direction of pattern motion (Movshon & Newsome, 1996; Rust, Mante, Simoncelli, & Movshon, 2006). There are three steps for the receptive-field shifts of the global motion detectors. First, component motions are detected in an early stage, for example in area V1. Second, global motion is identified in a later stage. Third, the receptive fields of the global motion detectors are shifted oppositely to the global motion identified by themselves.

What cortical mechanism might correspond to the functional construct, "global motion detectors"? For the conventional plaid motion used in Experiment 1, the pattern-motion cells in area MT would detect global motion. However, the cells of this type are only 25% of all MT neurons (Born & Bradley, 2005; Movshon & Newsome, 1996; Rust et al., 2006). Moreover, if two or more directions are presented simultaneously, as in the pseudo plaid pattern used in Experiment 2, in spatially separated positions within the receptive field, the pattern-motion cells in area MT exhibit a more component-motion-like tuning curve (Majaj et al., 2007). To identify the plaid motion and PPP motion correctly, population activity patterns rather than activities of single pattern-motion cells might be needed, and the pattern activities themselves might work as the neural mechanism of the spatial integration of motion information based on the intersection-of-constraints rule. Alternatively, these pattern activities might converge into a single neuron within a huge spatial summation property, such as neurons in area MST (Majaj et al., 2007; Perrone & Krauzlis, 2008), and this single neuron might be responsible for the perceived direction and position of a moving object.

No previous studies have examined whether the receptive fields of MT and MST neurons are shifted by global motion, however, some studies have shown that spatially flexible receptive fields exist in other areas, including the retina and area V4 (Berry, Brivanlou, Jordan, & Meister, 1999; Sundberg, Fallah, & Reynolds, 2006). For instance, Sundberg et al. (2006) revealed that the receptive fields of color-sensitive cells in area V4 were shifted in the direction opposite to the motion direction and argued that this property might mediate the visual phenomenon of motion assimilation of a stationary color flash by a moving stimulus (Cai & Schlag, 2001). As such, the shift of the receptive field in the direction opposite to visual motion direction might as well be found in many cortical areas including MT and MST. The dynamic property of flexible receptive fields might have the functional significance that each motion-sensitive cell could quickly respond to moving stimuli coming into the receptive field of the cell, leading to the potential benefit that the animal could react quickly to potential predators.

Acknowledgments

This research was supported by a Grant-in-Aid for Scientific Research No. 20020006 from MEXT, Japan.

Appendix A. Predicting MIPS for CG by MIPS for VG

Before Experiment 1, we measured the speed of the Plaid that appeared as fast as the VG moving at 0.8 deg/s. The speed-matching measurement was made independently under the three plaid-angle conditions and for all observers. Thus, the speed of the Plaid for each plaid-angle was different across individuals. Since the CG1 and CG2 were the separate presentations of the component gratings of a Plaid, their speed (denoted as "S_{CG}" below) also had different values across individuals.

To explain the MIPSs for the CG1 and CG2, we considered that these could be predicted by the orthogonal projection of the illusory position shift in the oblique direction of motion onto the horizontal axis of space. Because the CG1 and CG2 were obliquely oriented gratings, they would be perceptually shifted in their motion directions rather than in the horizontal direction. On the other hand, what we measured in the present psychophysical experiment was the horizontal component of illusory displacement. This is to say that what we actually measured was equivalent to the total MIPS for a single grating multiplied by cos θ, where θ indicates the angle between the global motion direction and each component grating's motion direction. If MIPS is proportional to speed (Bressler and Whitney, 2006; McGraw et al., 2002), then MIPS for a component grating should be estimated by

$$\mathrm{MIPS}_{CG} = \frac{S_{CG} \times \mathrm{MIPS}_{VG}}{S_{VG}} \times \cos\theta$$

where SCG indicates the speed of the CG1 and CG2, MIPSVG indicates the measured MIPS for the VG, and SVG indicates the speed of the VG (0.8 deg/s). Fig. A shows a scatterplot of the predicted MIPS against the measured MIPS for the CG1 and CG2 under all plaid-angle conditions and for all observers. The open circles indicate the CG1 data and the filled squares indicate the CG2 data. The linear regression analysis revealed that the slope of the regression line (solid line) was highly significant ($y = 0.98x - 0.42$; $R2 = 0.89$, $t = 15.02$, $p < .001$). Interestingly, the coefficient of the regression line was near 1, which means that the above calculation gives a reasonable approximation of the measured MIPS for the CG1 and CG2.

Appendix B. Predicting MIPS for PPP by MIPSs for local patches

In Experiment 2, the local horizontal MIPSs could also be calculated by the cosine function of θ as in Experiment 1, where θ indicates the angle between the global motion direction and each local patch's motion direction. We measured the MIPS for a single vertical Gabor patch of the same size as each component patch of the

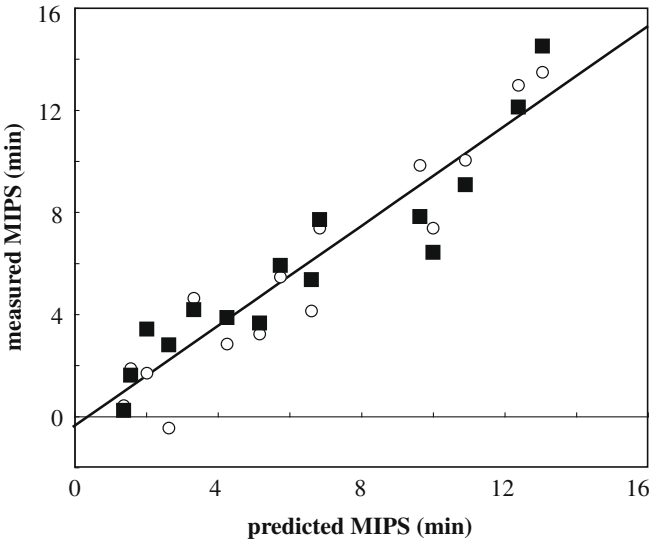

Fig. A. The scatterplot of the measured MIPS and predicted MIPS for the CG1 (open circles) and CG2 (filled squares) for all observers and all plaid-angle conditions in Experiment 1. The solid line is the linear regression line.

PPP (see Section 3.2). This local MIPS measurement was done at 1, 2, and 4 deg/s to obtain the speed-dependence curve (with linear interpolation) of the local MIPS. From the measured MIPS for this patch, we estimated the horizontal "MIPS" for each of the obliquely oriented component patches that comprised a PPP, in the following way. First, because the speed of each component patch obeyed the cosine function of θ, or the intersection-of-constraints rule, the physical speed of each component was the cosine function of θ. Second, in reference to the above speed-dependence curve, we estimated the MIPS that would occur in the direction of the motion of each patch moving at the above speed. Third, because each patch moved obliquely, the horizontal component of MIPS should be equal to the orthogonal projection of the true MIPS in the oblique direction onto the horizontal axis of space, and should obey the cosine function of θ.

References

Adelson, E. H., & Movshon, J. A. (1982). Phenomenal coherence of moving visual patterns. *Nature, 300*, 523–525.

Amano, K., Edwards, M., Badcock, D., & Nishida, S. (2009). Adaptive pooling of visual motion signals by the human visual system revealed with a novel multi-element stimulus. *Journal of Vision, 9*, 1–25.

Arnold, D. H., Thompson, M., & Johnston, A. (2007). Motion and position coding. *Vision Research, 47*, 2403–2410.

Berry, M. J., II, Brivanlou, I. H., Jordan, T. A., & Meister, M. (1999). Anticipation of moving stimuli by the retina. *Nature, 398*, 334–338.

Born, R. T., & Bradley, D. C. (2005). Structure and function of visual area MT. *Annual Review Neuroscience, 28*, 157–189.

Bowns, L. (1996). Evidence for a feature tracking explanation of why type II plaids move in the vector sum direction at short durations. *Vision Research, 36*, 3685–3694.

Braddick, O. (1984). Visual hyperacuity. *Nature, 308*, 228–229.

Bradley, D. C., & Goyal, M. S. (2008). Velocity computation in the primate visual system. *Nature Review Neuroscience, 9*, 686–695.

Bressler, D. W., & Whitney, D. (2006). Second-order motion shifts perceived position. *Vision Research, 46*, 1120–1128.

Bullier, J. (2001). Feedback connections and conscious vision. *Trends in Cognitive Sciences, 5*, 369–370.

Burke, D., Alais, D., & Wenderoth, P. (1994). A role for a low level mechanism in determining plaid coherence. *Vision Research, 34*, 3189–3196.

Cai, R., & Schlag, J. (2001). A new form of illusory conjunction between color and shape. *Journal of vision, 1*, 127a.

Carney, T., & Klein, S. A. (1999). Optimal spatial localization is limited by contrast sensitivity. *Vision Research, 39*, 503–511.

Chung, S. T., Patel, S. S., Bedell, H. E., & Yilmaz, O. (2007). Spatial and temporal properties of the illusory motion-induced position shift for drifting stimuli. *Vision Research, 47*, 231–243.

De Valois, R. L., & De Valois, K. K. (1991). Vernier acuity with stationary moving Gabors. *Vision Research, 31*, 1619–1626.

Derrington, A. M., Badcock, D. R., & Henning, G. B. (1993). Discriminating the direction of second-order motion at short stimulus durations. *Vision Research, 33*, 1785–1794.

Durant, S., & Zanker, J. M. (2009). The movement of motion-defined contours can bias perceived position. *Biology Letters, 5*, 270–273.

Edwards, M., & Badcock, D. R. (2003). Motion distorts perceived depth. *Vision Research, 43*, 1799–1804.

Fu, Y. X., Djupsund, K., Gao, H., Hayden, B., Shen, K., & Dan, Y. (2002). *Temporal specificity in the cortical plasticity of visual space representation*. Science.

Fu, Y. X., Shen, Y., Gao, H., & Dan, Y. (2004). Asymmetry in visual cortical circuits underlying motion-induced perceptual mislocalization. *The Journal of Neuroscience, 24*, 2165–2171.

Gegenfurtner, K. R. (2003). Cortical mechanisms of colour vision. *Nature Review Neuroscience, 4*, 563–572.

Harp, T. D., Bressler, D. W., & Whitney, D. (2007). Position shifts following crowded second-order motion adaptation reveal processing of local and global motion without awareness. *Journal of Vision, 7*, 1–13.

Hayes, A. (2000). Apparent position governs contour-element binding by the visual system. *Proceedings of the Royal Society, Series B, 267*, 1341–1345.

Kim, J., & Wilson, H. R. (1993). Dependence of plaid motion coherence on component grating directions. *Vision Research, 33*, 2479–2489.

Lu, Z. L., & Sperling, G. (1995). The functional architecture of human visual motion perception. *Vision Research, 35*, 2697–2722.

Majaj, N. J., Carandini, M., & Movshon, J. A. (2007). Motion integration by neurons in macaque MT is local, not global. *The Journal of Neuroscience, 27*, 366–370.

McGraw, P. V., Walsh, V., & Barrett, B. T. (2004). Motion-sensitive neurones in V5/MT modulate perceived spatial position. *Current Biology, 14*, 1090–1093.

McGraw, P. V., Whitaker, D., Skillen, J., & Chung, S. T. (2002). Motion adaptation distorts perceived visual position. *Current Biology, 12*, 2042–2047.

Morgan, M. J., Ward, R. M., & Hole, G. J. (1990). Evidence for positional coding in hyperacuity. *Journal of Optical Society of America A, 7*, 297–304.

Movshon, J. A., & Newsome, W. T. (1996). Visual response properties of striate cortical neurons projecting to area MT in macaque monkeys. *The Journal of Neuroscience, 16*, 7733–7741.

Murakami, I., & Kashiwabara, Y. (2009). Illusory position shift induced by cyclopean motion. *Vision Research, 49*, 2037–2043.

Mussap, A. J., & Prins, N. (2002). On the perceived location of global motion. *Vision Research, 42*, 761–769.

Nijhawan, R. (1994). Motion extrapolation in catching. *Nature, 370*, 256–257.

Nijhawan, R. (1997). Visual decomposition of colour through motion extrapolation. *Nature, 386*, 66–69.

Nishida, S., Amano, K., Edwards, M., & Badcock, D. R. (2006). Global motion with multiple Gabors: A tool to investigate motion integration across orientation and space. *Journal of Vision, 6*, 1084a.

Nishida, S., & Johnston, A. (1999). Influence of motion signals on the perceived position of spatial pattern. *Nature, 397*, 610–612.

Nishida, S., & Sato, T. (1995). Motion aftereffect with flickering test patterns reveals higher stages of motion processing. *Vision Research, 35*, 477–490.

Patel, S. S., Bedell, H. E., & Ukwade, M. T. (1999). Vernier judgments in the absence of regular shape information. *Vision Research, 39*, 2349–2360.

Pavan, A., & Mather, G. (2008). Distinct position assignment mechanisms revealed by cross-order motion. *Vision Research, 48*, 2260–2268.

Perrone, J. A., & Krauzlis, R. J. (2008). Spatial integration by MT pattern neurons: A closer look at pattern-to-component effects and the role of speed tuning. *Journal of Vision, 8*, 11–14.

Ramachandran, V. S., & Anstis, S. M. (1990). Illusory displacement of equiluminous kinetic edges. *Perception, 19*, 611–616.

Rider, A., & Johnston, A. (2009). Motion-induced position shifts are based on global motion estimates. *Journal of Vision, 9*, 655a.

Rust, N. C., Mante, V., Simoncelli, E. P., & Movshon, J. A. (2006). How MT cells analyze the motion of visual patterns. *Nature Neuroscience, 9*, 1421–1431.

Scase, M. O., Braddick, O. J., & Raymond, J. E. (1996). What is noise for the motion system? *Vision Research, 36*, 2579–2586.

Shim, W. M., & Cavanagh, P. (2004). The motion-induced position shift depends on the perceived direction of bistable quartet motion. *Vision Research, 44*, 2393–2401.

Shipp, S., & Zeki, S. (1989a). The organization of connections between areas V5 and V1 in macaque monkey visual cortex. *European Journal of Neuroscience, 1*, 309–332.

Shipp, S., & Zeki, S. (1989b). The organization of connections between areas V5 and V2 in macaque monkey visual cortex. *European Journal of Neuroscience, 1*, 333–354.

Snowden, R. J. (1998). Shifts in perceived position following adaptation to visual motion. *Current Biology, 8*, 1343–1345.

Solomon, S. G., & Lennie, P. (2007). The machinery of colour vision. *Nature Review Neuroscience, 8*, 276–286.

Sperling, G. (1998). First-order, second-order, and third-order motion systems. *Perception, 27*(Suppl. 3) [ECVP abstract].

Sundberg, K. A., Fallah, M., & Reynolds, J. H. (2006). A motion-dependent distortion of retinotopy in area V4. *Neuron, 49*, 447–457.

Takeuchi, T. (1998). Effect of contrast on the perception of moving multiple Gabor patterns. *Vision Research, 38*, 3069–3082.

Tsui, S. Y., Khuu, S. K., & Hayes, A. (2007a). Apparent position in depth of stationary moving three-dimensional objects. *Vision Research, 47*, 8–15.

Tsui, S. Y., Khuu, S. K., & Hayes, A. (2007b). The perceived position shift of a pattern that contains internal motion is accompanied by a change in the pattern's apparent size and shape. *Vision Research, 47*, 402–410.

Watanabe, K., Nijhawan, R., & Shimojo, S. (2002). Shifts in perceived position of flashed stimuli by illusory object motion. *Vision Research, 42*, 2645–2650.

Welch, L. (1989). The perception of moving plaids reveals two motion-processing stages. *Nature, 337*, 734–736.

Westheimer, G. (1975). Visual acuity and hyperacuity. *Investigative Ophthalmology, 14*, 570–572.

Whitney, D. (2002). The influence of visual motion on perceived position. *Trends in Cognitive Sciences, 6*, 211–216.

Whitney, D. (2005). Motion distorts perceived position without awareness of motion. *Current Biology, 15*, R324–326.

Whitney, D., & Cavanagh, P. (2000). Motion distorts visual space: Shifting the perceived position of remote stationary objects. *Nature Neuroscience, 3*, 954–959.

Whitney, D., Goltz, H. C., Thomas, C. G., Gati, J. S., Menon, R. S., & Goodale, M. A. (2003). Flexible retinotopy: Motion-dependent position coding in the visual cortex. *Science, 302*, 878–881.